

Formulation of Small Activating RNA Into Lipidoid Nanoparticles Inhibits Xenograft Prostate Tumor Growth by Inducing p21 Expression

Robert F Place^{1,2}, Ji Wang¹, Emily J Noonan^{3,4}, Rachel Meyers⁵, Muthiah Manoharan⁵, Klaus Charisse⁵, Rick Duncan⁵, Vera Huang¹, Xiaoling Wang¹ and Long-Cheng Li¹

Application of RNA interference (RNAi) in the clinic has improved with the development of novel delivery reagents (e.g., lipidoids). Although RNAi promises a therapeutic approach at silencing gene expression, practical methods for enhancing gene production still remain a challenge. Previously, we reported that double-stranded RNA (dsRNA) can activate gene expression by targeting promoter sequence in a phenomenon termed RNA activation (RNAa). In the present study, we investigate the therapeutic potential of RNAa in prostate cancer xenografts by using lipidoid-based formulation to facilitate *in vivo* delivery. We identify a strong activator of gene expression by screening several dsRNAs targeting the promoter of tumor suppressor p21^{WAF1/Cip1} (p21). Chemical modification is subsequently implemented to improve the medicinal properties of the candidate duplex. Lipidoid-encapsulated nanoparticle (LNP) formulation is validated as a delivery vehicle to mediate p21 induction and inhibit growth of prostate tumor xenografts grown in nude mice following intratumoral injection. We provide insight into the stepwise creation and analysis of a putative RNAa-based therapeutic with antitumor activity. Our results provide proof-of-principle that RNAa in conjunction with lipidoids may represent a novel approach for stimulating gene expression *in vivo* to treat disease.

Molecular Therapy–Nucleic Acids (2012) 1, e15; doi:10.1038/mtna.2012.5; advance online publication 27 March 2012

Introduction

RNA interference (RNAi) is an evolutionarily conserved mechanism of gene regulation by which small double-stranded RNA (dsRNA) molecules—termed small interfering RNAs (siRNAs)—degrade complementary messenger RNA to silence gene expression.¹ By using siRNAs as therapeutic compounds, it is possible to block the production of disease-causing proteins. As such, RNAi is being implemented in clinical trials for the treatment of a variety of diseases (e.g., hypercholesterolemia, cancer, etc.).²

Lipidic-based vectors are the preferred approach for siRNA delivery *in vitro* and *in vivo*. Precise formulation of siRNAs with lipid, polyethylene glycol-lipid, and cholesterol allows encapsulation into liposomal nanoparticles for improved bioavailability.³ Although this method is preferably utilized to target the liver, lipid formulations have been applied to efficiently deliver siRNA to solid tumors in mice.⁴ Further development has also led to an enhanced class of lipid-like molecules—termed lipidoids—with refined delivery functions.^{5,6} Currently, lipidoid 95N₁₂-5(1) is considered a leading material for effective *in vivo* delivery of siRNA.

Safe strategies to selectively enhance gene and/or protein production remain a challenge in gene therapy. Viral-based systems have inherent drawbacks including adverse effects

on host genome integrity, immunological consequences, etc. Recently, small dsRNAs have also been shown to induce gene expression in a phenomenon referred to as RNA activation (RNAa).^{7–10} Several models of RNAa have been described including transcriptional activation by targeting promoter sequences^{7,8,11,12} and/or overlapping noncoding transcripts.^{13–15} This technique offers a similar approach as RNAi, while representing a new strategy to stimulate gene expression.

Cyclin-dependent kinase (CDK) inhibitor p21^{WAF1/CIP1} (p21) is a mediator of several anti-growth pathways including cell cycle arrest.¹⁶ The effects of p21 are partially mediated through the retinoblastoma (Rb) protein, which is inactivated in proliferating cells by phosphorylation.¹⁷ By directly suppressing CDK activity, p21 promotes Rb hypophosphorylation leading to cell cycle arrest. In normal cells, p21 participates in several cellular processes including controlled growth, differentiation, and senescence.^{16,18,19} However, p21 is considered a potent tumor suppressor gene in cancer cells.²⁰ Ectopic expression of p21 has been shown to inhibit tumor growth both *in vitro* and *in vivo*, as well as induce apoptosis.^{21,22}

Disruption of the Rb pathway is frequent in human cancers²³; however, loss-of-function mutations to p21 are generally a rare occurrence.^{24–26} In this regard, p21 may be an ideal target for RNAa to inhibit tumor cell growth. Although

¹Department of Urology and Helen Diller Comprehensive Cancer Center, University of California, San Francisco, California, USA; ²RNA Therapeutics, Inc., San Francisco, California, USA; ³Center for Molecular Biology in Medicine, Veterans Affairs Palo Alto Health Care System, Palo Alto, California, USA; ⁴Department of Medicine, Stanford University School of Medicine, Stanford, California, USA; ⁵Alnylam Pharmaceuticals, Inc., Cambridge, Massachusetts, USA

Correspondence: Robert F Place, Helen Diller Comprehensive Cancer Center, 1450 3rd St., HD383, San Francisco, California 94158, USA.

E-mail: place.robert@gmail.com or Long-Cheng Li, Helen Diller Comprehensive Cancer Center, 1450 3rd St., HD383, San Francisco, California 94158, USA.

E-mail: lilc@urology.ucsf.edu

Keywords: CDKN1A; delivery; gene activation; gene therapy; lipid nanoparticles; prostate cancer; saRNA; siRNA

Received 11 February 2012; revised 15 February 2012; accepted 15 February 2012

previous studies have implemented this technique *in vitro*,^{27,28} it is unclear if RNAa is applicable *in vivo* using clinically relevant delivery systems. In the present study, we screen several dsRNAs in order to identify a strong activator of p21 expression for *in vivo* delivery into human prostate xenograft tumors. We provide insight into the stepwise creation of a candidate dsRNA with improved medicinal properties and potent antiproliferative effects in prostate cancer cells. Additional molecular experiments assess sequence requirement and validate the dependency of growth inhibition on p21 induction. Subsequent delivery assays reveal lipidoid-based formulation mediates p21 induction and suppresses xenograft tumor growth. Our results provide proof-of-principle that lipidoids have application in delivering RNA duplexes *in vivo* to facilitate RNAa, as well as highlight a candidate RNAa-based drug with antitumor activity.

Results

Characterization of chemically modified dsRNA designed to induce p21 expression

It has been previously reported that p21 is susceptible to gene induction by targeting promoter sequence with dsRNA.⁷ In order to identify a strong activator of p21, we designed several dsRNAs according to published design rules^{7,11} that targeted sites -208, -254, -280, -322, -365, -402, -422, and -466 bp relative to the p21 transcription start site (Figure 1a). Each duplex was named according to its target within the p21 promoter (*i.e.*, dsP21-208, dsP21-254, etc.). A nonspecific dsRNA (dsCon) was also synthesized to serve as a control. Each duplex was transfected into PC-3 (prostate adenocarcinoma) cells and gene expression was evaluated 72 hours later. As shown in Figure 1b,c, dsP21-365 and dsP21-422 did not significantly augment p21 expression; however, dsP21-254, dsP21-280, dsP21-322, and dsP21-402 resulted in variable levels of gene induction. Conversely, both dsP21-208 and dsP21-466 had a reciprocal effect downregulating p21 expression by ~80%—a feature reminiscent of transcriptional gene silencing mediated by small RNA²⁹ (Figure 1b,c). Overall, dsP21-322 was the strongest activator of p21 expression elevating levels in excess of 14-fold (Figure 1b,c). As such, dsP21-322 was selected for further evaluation.

Chemical modification is often required to improve the efficacy and medicinal properties of duplex RNAs. Modification to the 2' position in the ribose backbone (*e.g.*, 2'-fluoro) is utilized to improve nuclease resistance and reduce stimulation of the innate immune response.³⁰ To improve the medicinal features of dsP21-322, we created a fully modified dsP21-322 (dsP21-322-2'F-S/AS) in which all cytosine and uridine nucleosides within the duplex contained a 2'-fluoro-modified ribose sugar (Supplementary Figure S1a). However, dsP21-322-2'F-S/AS suffered from inferior function as it possessed less than half the activity of dsP21-322 (Supplementary Figure S1b). It has been previously reported that excessive modification to the passenger strand in dsRNA molecules can interfere with RNAa activity.³¹ As such, we synthesized another modified dsP21-322 (dsP21-322-2'F) in which only the cytidines and uridines in the antisense strand—previously identified as the guide strand³¹—contained 2'-fluoro-modifications (Figure 2a). Transfection of dsP21-322-2'F induced p21 expression to

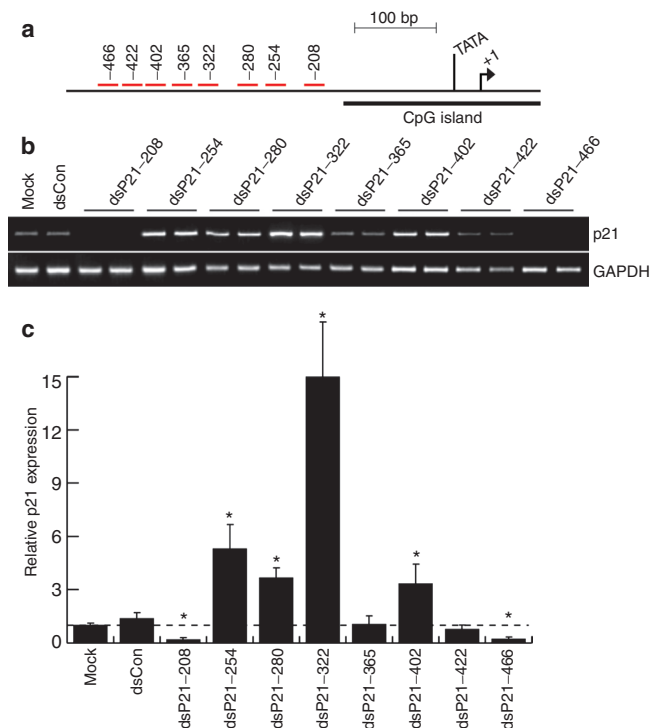


Figure 1 Promoter-targeting dsRNA and p21 expression. (a) Schematic representation of the p21 promoter including CpG island and TATA box. Indicated are the locations of each dsRNA target site relative to the transcription start site (+1). (b) PC-3 cells were transfected at 50 nmol/l concentrations of the indicated duplexes for 72 hours. Mock samples were transfected in the absence of dsRNA. Expression levels of p21 and GAPDH were assessed by semi-quantitative RT-PCR. GAPDH served as a loading control. (c) Relative expression of p21 was determined by real-time PCR (mean \pm SD from three independent experiments). Values of p21 were normalized to GAPDH. The dotted line represents baseline levels. Statistical significance was determined by two-tailed *t*-test against control treatments ($*P < 0.01$). dsRNA, double-stranded RNA; GAPDH, glyceraldehyde 3-phosphate dehydrogenase; RT-PCR, reverse transcription-PCR.

levels similar to unmodified dsP21-322 (Figure 2b,c). Immunoblot analysis also confirmed an increase in p21 protein levels (Figure 2d). Because PC-3 cells possess wild-type Rb protein that is inactivated by hyperphosphorylation,³² we also evaluated Rb phosphorylation status. As shown in Figure 2d, dsP21-322 and dsP21-322-2'F caused a considerable reduction in phosphorylated Rb (P-Rb) levels suggesting p21 activation results in a fully functional protein capable of manipulating Rb activity.

To test the medicinal benefits of dsP21-322-2'F, we evaluated its nuclease sensitivity in active mouse serum. As shown in Figure 2e, dsP21-322-2'F was stable for up to 8 hours in serum compared to unmodified dsP21-322. Even at 24 hours, low levels of dsP21-322-2'F duplex remained detectable (Figure 2e). Quantification of duplex decay estimated the half-life of dsP21-322-2'F to be ~14 hours, while dsP21-322 was only ~6 hours (Supplementary Figure S2). To evaluate its immune stimulatory effects, human peripheral blood mononuclear cells isolated from donor patients were transfected with dsP21-322-2'F and tested for IFN- α and

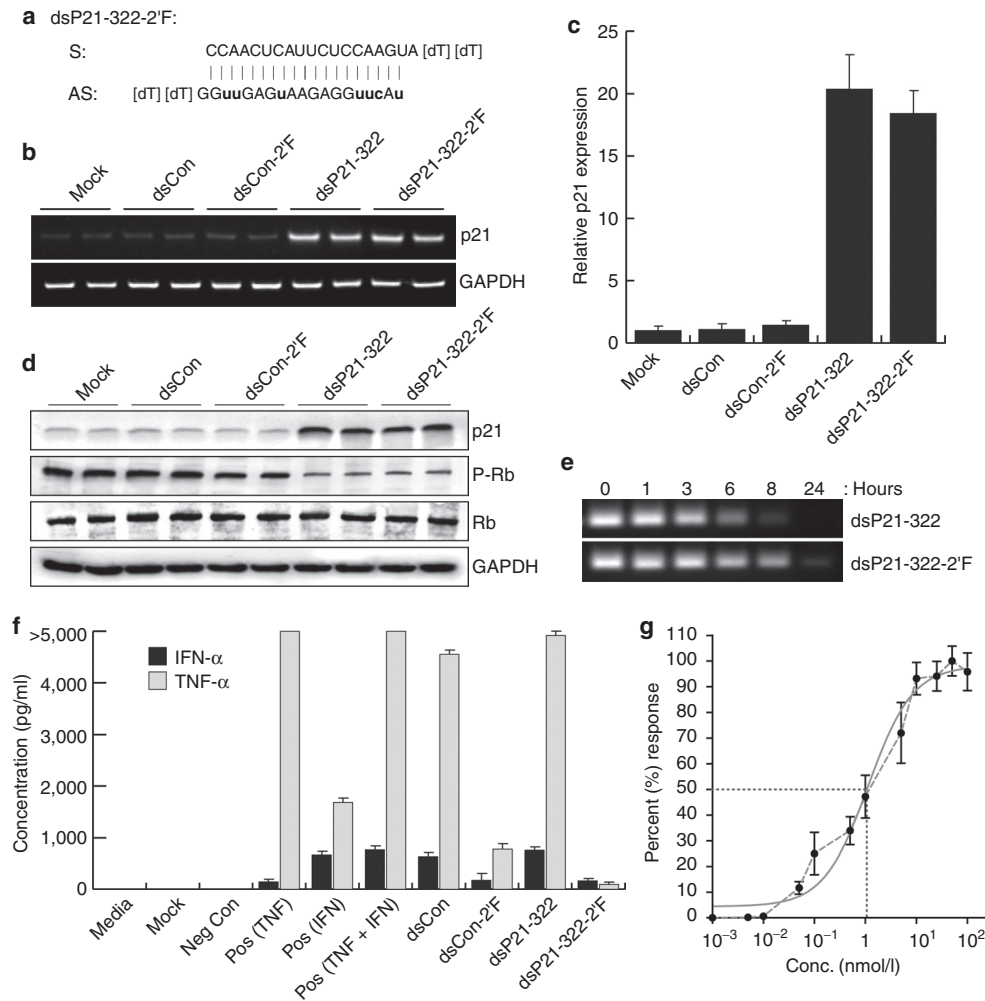


Figure 2 Activity and medicinal properties of dsP21-322-2'F. (a) Sequence composition of dsP21-322-2'F. Indicated are the sense (S) and antisense (AS) strands, which possess dual deoxythymidine overhangs at their 3'-termini. Lowercase letters in bold correspond to 2'-fluoro-modified nucleotides. (b) PC-3 cells were transfected at 50 nmol/l concentrations of dsCon, dsCon-2'F, dsP21-322, or dsP21-322-2'F for 72 hours. Mock samples were transfected in the absence of dsRNA. Expression levels of p21 and GAPDH were assessed by semi-quantitative RT-PCR. GAPDH served as a loading control. (c) Relative expression of p21 was determined by real-time PCR (mean \pm SD from three independent experiments). Values of p21 were normalized to GAPDH. (d) Protein levels of p21, phosphorylated Rb (P-Rb), total Rb, and GAPDH were evaluated by immunoblot analysis using protein-specific antibodies. (e) Equal quantities of dsP21-322 and dsP21-322-2'F were diluted in active mouse serum and incubated at 37 °C for the indicated lengths time. Duplex stability was visualized on an agarose gel. (f) Human PBMC cells were transfected with 133 nmol/l concentrations of each indicated dsRNAs for 24 hours. Levels of IFN- α and TNF- α were assessed by ELISA. Known strong activators of IFN- α (IFN) and/or TNF- α (TNF) served as positive controls (Pos). A duplex with no immune stimulatory effect acted as a negative control (Neg Con). Results from the most responsive donor are shown. (g) PC-3 cells were transfected with accumulating concentrations of dsP21-322-2'F for 72 hours. Expression of p21 was quantified by real-time PCR (mean \pm SD from two independent experiments). Maximum and minimum levels of induction correlate to 100 and 0% response, respectively. Nonlinear regression analysis was utilized to generate best fit line. Duplex concentration is shown in log scale. Dotted lines illustrate approximate EC_{50} . dsRNA, double-stranded RNA; EC_{50} , half maximal effective concentration; ELISA, enzyme-linked immunosorbent assay; GAPDH, glyceraldehyde 3-phosphate dehydrogenase; IFN- α , interferon- α ; PBMC, peripheral blood mononuclear cell; Rb, retinoblastoma; RT-PCR, reverse transcription-PCR; TNF- α , tumor necrosis factor- α .

tumor necrosis factor- α (TNF- α) production by enzyme-linked immunosorbent assay. Several duplexes previously identified to be strong activators of IFN- α and/or TNF- α were utilized as positive controls, while another duplex with no immune stimulatory effect was used as a negative control.^{33,34} As shown in **Figure 2f**, unmodified dsCon and dsP21-322 induced robust IFN- α and TNF- α production similar to the positive controls, while cytokine stimulation was tremendously reduced in dsP21-322-2'F and dsCon-2'F treatments. Taken together,

these results indicate that dsP21-322-2'F possesses activity similar to its unmodified form with enhanced nuclease stability and reduced immune stimulatory effects.

To characterize dsP21-322-2'F potency, we calculated its EC_{50} (half maximal effective concentration) value by measuring p21 expression levels following transfection at accumulating concentrations in PC-3 cells. Percent response was determined by setting the maximum and minimum p21 expression values to 100 and 0% activity, respectively. As

shown in **Figure 2g**, the estimated EC₅₀ of dsP21-322-2'F was ~1 nmol/l in PC-3 cells at 72 hours.

Inhibition of prostate cancer cell growth by dsP21-322-2'F

Overexpression of p21 is known to suppress cell proliferation, as well as promote cell death.^{21,22} Quantitative analysis by MTS assay revealed that cell viability steadily decreased following dsP21-322-2'F transfection in PC-3 cells (**Figure 3a**). Elevated and sustained expression of p21 correlated with reduced viability by dsP21-322-2'F (**Supplementary Figure S3a,b**). Cells also appeared less dense and displayed larger, flattened morphologies that continued to enlarge by day 7; phenotypes indicative of impeded cell growth (**Supplementary Figure S3c**). Clonogenicity assays also revealed that dsP21-322-2'F prevented colony formation compared to control treatments (**Figure 3b**).

To evaluate cell cycle distribution, DNA content was analyzed by flow cytometry in cells stained with propidium iodide following dsP21-322-2'F transfection. As shown in **Figure 3c,d**,

dsP21-322-2'F caused G₀/G₁ arrest in PC-3 cells as indicated by the increase in G₀/G₁ cell number and concurrent declines in S and G₂/M populations. Further analysis of the entire gated whole-cell population revealed a significant increase in the subdiploid fraction of dsP21-322-2'F-treated cells suggestive of DNA fragmentation and cell death (**Figure 3c,d**).

Overexpression of p21 has also been linked to cellular senescence.^{18,19} To evaluate induced senescence, PC-3 cells were transfected with dsP21-322-2'F and stained for senescence-associated β -galactosidase (SA- β -gal) activity. As shown in **Figure 3e**, PC-3 cells stained positive for SA- β -gal activity following dsP21-322-2'F treatment. In contrast, SA- β -gal staining in mock and dsCon-2'F treatments were nearly undetectable.

Susceptibility to p21 induction and inhibition of cell growth by dsP21-322-2'F was also assessed in prostate cancer cell lines with different genetic backgrounds including DU-145 (prostate carcinoma) and LNCaP (prostate adenocarcinoma) cells. Analysis of messenger RNA expression revealed that p21 levels increased by five and fourfold in LNCaP and DU-145 cells, respectively (**Supplementary Figure S4a,b**).

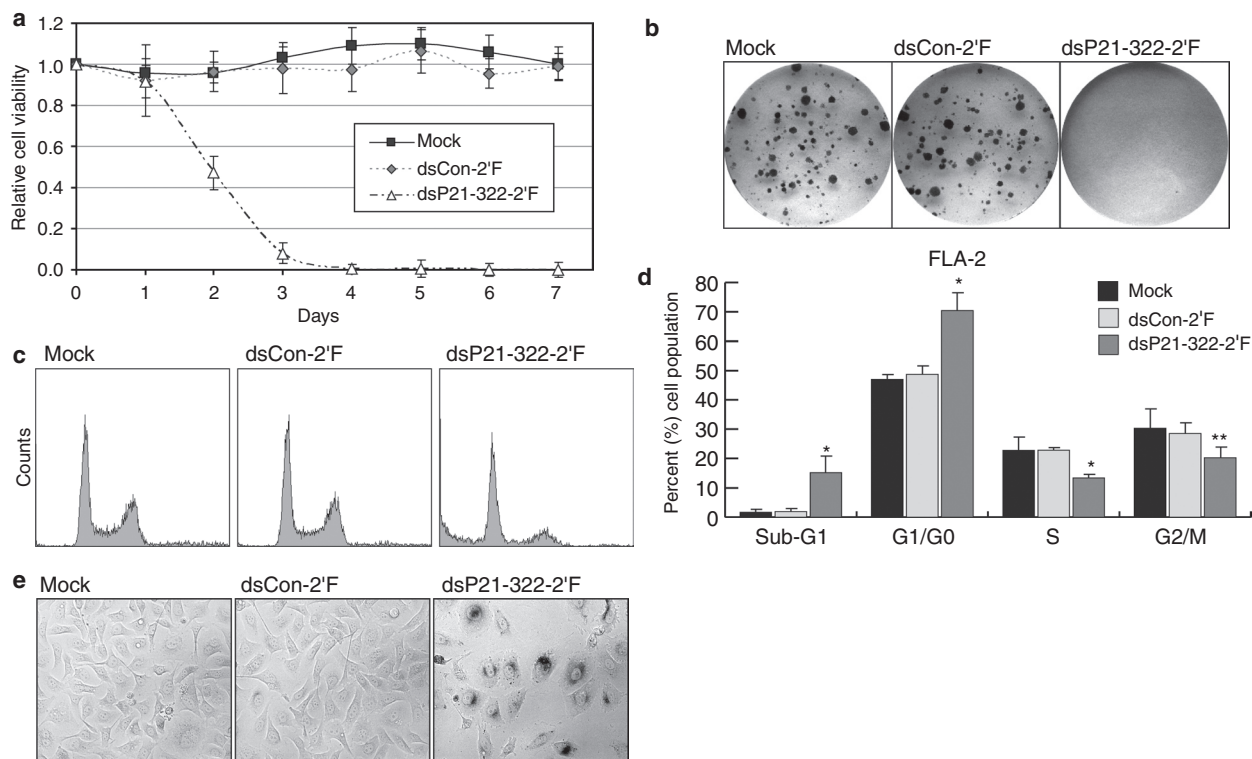


Figure 3 dsP21-322-2'F reduces prostate cancer cell viability and growth. (a) PC-3 cells were transfected with 50 nmol/l concentrations of dsCon-2'F or dsP21-322-2'F and seeded in 96-well microplates. Mock samples were transfected in the absence of dsRNA. Cell viability was quantified at each day utilizing MTS reagent. Data is plotted as the mean \pm SE of two independent experiments relative to untreated cells. (b) PC-3 cells were plated at ~2,500 cells in 30 mm tissue culture dishes and transfected the following day. Cells were grown for ~11 days and analyzed for colony formation by staining with crystal violet. Shown are representative photographs taken of tissue culture plates from each treatment group. (c) PC-3 cells were transfected with mock, dsCon-2'F, or dsP21-322-2'F for 72 hours. Floating and attached cells were collected, stained with PI, and processed for analysis by flow cytometry to measure DNA content. Shown are examples of resulting FLA2 histograms. (d) Flow cytometry data was analyzed to determine cell cycle distribution (mean \pm SD from four independent experiments). Percentages of sub-G1 cells were calculated from entire gated whole-cell populations, whereas cell cycle distribution (G₀/G₁, S, and G₂/M) was determined from only surviving cells. Statistical significance was determined by two-tailed *t*-test against control treatments (**P* < 0.01; ***P* < 0.05). (e) PC-3 cells were transfected with dsRNA for 3 days, fixed in formaldehyde, and stained for SA- β -gal activity overnight. Images were captured by bright field microscopy at $\times 200$ magnification. Dark perinuclear staining marks senescent cells. dsRNA, double-stranded RNA; MTS, 3-(4,5-dimethylthiazol-2-yl)-5-(3-carboxymethoxyphenyl)-2-(4-sulfophenyl)-2H-tetrazolium; PI, propidium iodide; SA- β -gal, senescence-associated β -galactosidase.

In addition, dsP21-322-2'F also caused a steady reduction in LNCaP and DU-145 cell viability (**Supplementary Figure S4c**). Taken together, these results indicate that dsP21-322-2'F has putative antitumor activity in several different prostate cancer cell lines.

Sequence requirement of dsP21-322-2'F

To test the general sensitivity of p21 to nonspecific sequences, we blindly screened 11 additional RNA duplexes (dsRNA-1 to dsRNA-11) with defined and undefined activities for the capability to induce p21 levels. Overall, p21 was not responsive to nonspecific duplex treatment; only dsRNA-4 and dsRNA-8 minimally increased p21 levels by approximately two to threefold (**Supplementary Figure S5a**). This data suggests that activation of p21 is not a general consequence of dsRNA treatment, but rather specific to the sequence of dsP21-322-2'F.

To define the sequence requirement of dsP21-322-2'F, several mismatched mutants (dsP21-322-MM1 to dsP21-322-MM9) were synthesized and evaluated for the ability to activate p21 expression. Each mutant possessed three tandem nucleotide mismatches relative to the intended target site in the p21 promoter that partially overlapped with the mutation site in the preceding mutant duplex (**Supplementary Figure S5b**). As shown in **Supplementary Figure S5c**, none of the mutant derivatives possessed heightened activity. Rather, mutation within the "seed" sequence (dsP21-322-MM3) and 3'-flanking region (dsP21-322-MM6 and dsP21-322-MM7) completely prevented p21 induction, while mismatches corresponding to the center (dsP21-322-MM5) and 3'-terminal end (dsP21-322-MM9) of the duplex had no impact on activity. In addition, the remaining duplexes (dsP21-322-MM1, dsP21-322-MM2, dsP21-322-MM4, and dsP21-322-MM8) all possessed reduced function (**Supplementary Figure S5c**). Based on this data, two internal sequences roughly corresponding to nucleotides 1–7 and 12–16 relative to the 5'-end of the antisense strand are required for optimal induction of p21 (**Supplementary Figure S5d**).

Growth inhibition of dsP21-322-2'F is dependent on p21 induction

Mutant derivatives (**Supplementary Figure S5b,c**) that retained mid-to-strong p21 induction activity (dsP21-322-MM1, dsP21-322-MM4, dsP21-322-MM5, dsP21-322-MM8, and dsP21-322-MM9) acquired morphological changes similar to dsP21-322-2'F (**Supplementary Figure S6a**). Duplexes with low (dsP21-322-MM2) or no capacity to activate p21 expression (dsP21-322-MM3, dsP21-322-MM6, and dsP21-322-MM7) correlated with minimal or no visible changes in cell phenotype, respectively (**Supplementary Figure S6a**). Quantitative analysis revealed that declines in cell viability also correlated to the capacity of dsP21-322-2'F and its mutant derivatives to activate p21 expression—dsP21-322-MM3 being the only derivative that had no impact on p21 induction, but retained a partial inhibitory function on PC-3 cell viability (**Supplementary Figure S6b**). Collectively, these results suggest that the growth inhibitory function of dsP21-322-2'F correlates with p21 induction.

Cotreatment with siRNA targeting p21 messenger RNA may be utilized to counteract p21 induction by dsP21-322-

2'F. As such, we designed and synthesized a highly effective siRNA (siP21) with an empirically calculated IC_{50} (half maximal inhibitory concentration) of 4 pmol/l (data not shown). Another siRNA (siCon) with no known RNAi activity was utilized as a control. Combination treatments of siP21 and dsP21-322-2'F were performed to identify a minimal effective concentration of siRNA to compensate for p21 induction. As shown in **Supplementary Figure S7a**, cotreatments with 0.5 nmol/l siP21 and ~10–15 nmol/l dsP21-322-2'F restored p21 expression to near basal levels at 72 hours. However, combination treatments with 0.5 nmol/l siCon interfered with dsP21-322-2'F activity reducing its EC_{50} by tenfold (**Supplementary Figure S7b,c**). Two additional siRNAs (siXBP and siSID1) with known function and calculated IC_{50} values similar to siP21 also interfered with dsP21-322-2'F activity in a manner similar to siCon suggesting co-delivery of multiple dsRNAs may interfere with RNAi activity (**Supplementary Figure S7d,e**).

In order to determine if blocking p21 induction by siRNA interferes with dsP21-322-2'F function, cotreatments were performed with 12 nmol/l dsP21-322 to compensate for 0.5 nmol/l siCon or siP21. As shown in **Figure 4a**, transfection of dsP21-322-2'F at the proper ratio with siP21 or siCon allowed for minimal changes in p21 expression or induction roughly equal to 1 nmol/l dsP21-322-2'F, respectively. Prevention of p21 induction by siP21 also appeared to partially interfere with the ability of dsP21-322-2'F to deplete P-Rb levels (**Figure 4b**). Further analysis revealed siP21 altered dsP21-322-2'F cell cycle distribution resulting in a profile that resembled control treatments; restoration in S phase population with corresponding depletion in G0/G1 cell number (**Figure 4c,d**). Analysis of the gated whole-cell population also revealed siP21 partially reduced the number of sub-G1 cells in dsP21-322-2'F treatments (**Figure 4c,d**). These results indicate that the growth inhibitory function of dsP21-322-2'F is dependent on p21 induction.

Off-target activities of dsP21-322-2'F

Global deregulation of other cell cycle-related genes and/or changes in upstream transcriptional regulators may result in p21 induction *via* nonspecific mechanisms. To investigate off-target activities of dsP21-322-2'F, we screened the expression of several cyclin transcripts (*i.e.*, CCND1, CCNA1, and CCNE1), CDK inhibitor family members (*i.e.*, p16, p15, and p27), and known transcriptional regulators of p21 (*i.e.*, SP1, SP3, Myc, E2F1, E2F3, and HDAC1) by real-time PCR.^{35,36} Upstream factor p53 was not evaluated because PC-3 cells are null for p53 expression.³² Of the 12 genes, dsP21-322-2'F caused increases in CCNE1, p15, and p27, as well as reduced HDAC1 expression (**Supplementary Figure S8a,b**). Deregulation in gene expression was not a downstream consequence of p21 activation as siP21 blocked p21 induction, but did not restore basal levels of CCNE1, p15, p27, or HDAC1 (**Supplementary Figure S8c,d**). Selective knockdown of HDAC1 by siRNA (siHDAC1) did not impact p21 expression; however, p15 and p27 levels were elevated by siHDAC1 (**Supplementary Figure S8e–g**). These results indicate dsP21-322-2'F possesses off-target activities; however, p21 activation is independent of HDAC1 depletion.

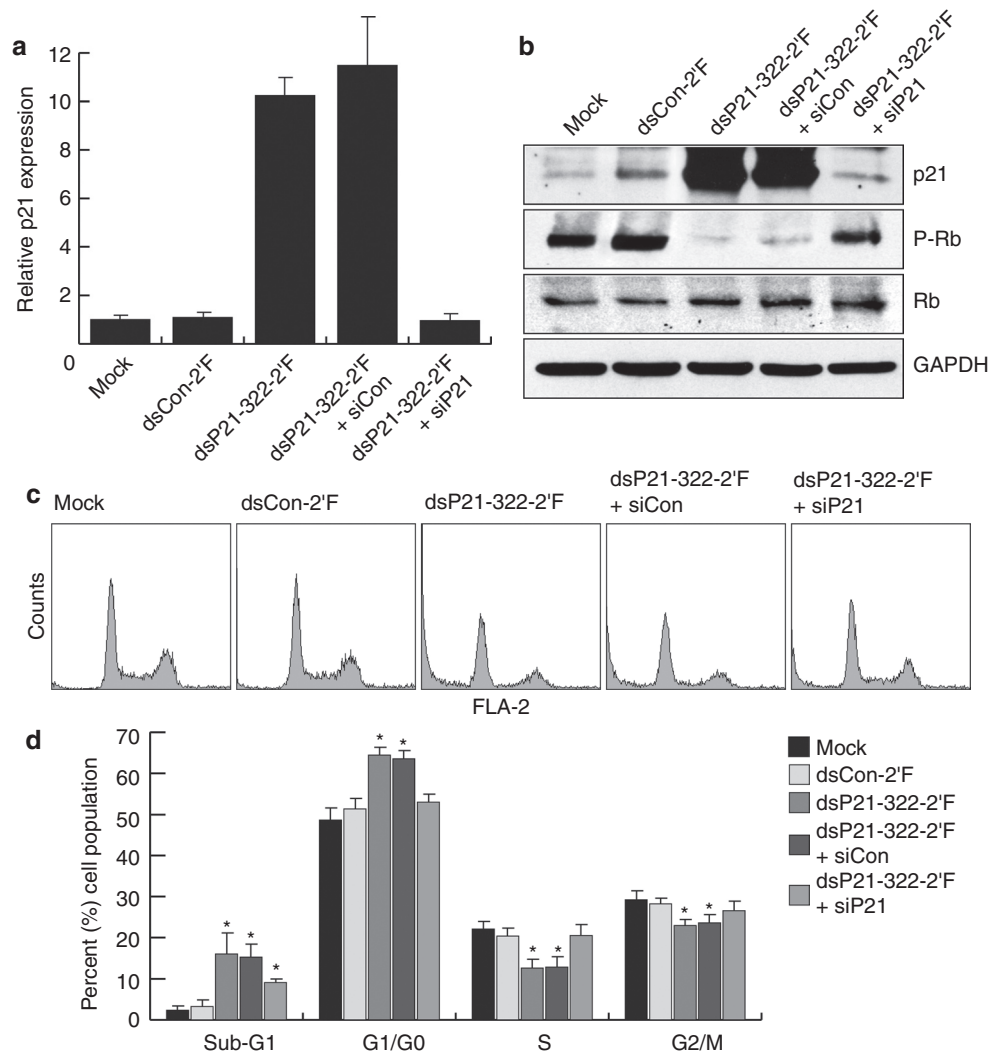


Figure 4 Growth inhibition of dsP21-322-2'F is dependent on p21 induction. (a) PC-3 cells were transfected at 1 nmol/l concentrations dsCon-2'F or dsP21-322-2'F for 72 hours. Cotreatments were performed at 0.5 nmol/l concentrations of siP21 or siCon in combination with 12 nmol/l dsP21-322-2'F. Relative expression of p21 was determined by real-time PCR (mean \pm SD from two independent experiments). Values of p21 were normalized to GAPDH. (b) Protein levels of p21, phosphorylated Rb (P-Rb), total Rb, and GAPDH were evaluated by immunoblot analysis using protein-specific antibodies. GAPDH served as a loading control. (c) Flowing and attached cells were collected, stained with PI, and processed for analysis by flow cytometry to measure DNA content. Shown are examples of resulting FLA-2 histograms. (d) Flow cytometry data was analyzed to determine cell cycle distribution (mean \pm SD from at least six independent experiments). Percentages of sub-G1 cells were calculated from entire gated whole-cell populations, whereas cell cycle distribution (G0/G1, S, and G2/M) was determined from only surviving cells. Statistical significance was determined by two-tailed *t*-test against control treatments ($*P < 0.01$). GAPDH, glyceraldehyde 3-phosphate dehydrogenase; PI, propidium iodide; Rb, retinoblastoma.

Lipidoid-mediated delivery of dsP21-322-2'F

Lipidoids are a class of liposomal-like molecules that have been screened for effective *in vivo* delivery of siRNA molecules.^{5,6} To determine if lipidoids are capable of mediating RNAa, lipidoid-encapsulated dsP21-322-2'F nanoparticles (LNP-dsP21-322-2'F) were generated with 95N₁₂-5(1) under parameters for maximal efficacy and tested *in vitro* for p21 induction. Nonspecific lipidoid-based nanoparticles (LNP-dsCon-2'F) were also formulated as a control. PC-3 cells were treated with 0–9 μ g/ml of LNP-dsP21-322-2'F or LNP-dsCon-2'F for 72 hours and p21 expression was evaluated by semi-quantitative and real-time PCR. Transfection of non-formulated dsRNA with RNAiMax was used as a positive control for *in vitro* activity.

Compared to LNP-dsCon-2'F, LNP-dsP21-322-2'F incrementally elevated p21 levels relative to particle concentration; doses at 9 μ g/ml roughly equaled levels in RNAiMax treatments (Figure 5a,b). Direct analysis of cellular uptake revealed LNP-dsP21-322-2'F at 9 μ g/ml effectively delivered dsP21-322-2'F to levels comparable to RNAiMax (Supplementary Figure S9). Cumulative reductions in cell viability also correlated to the incremental increases in p21 expression (Figure 5c). By day 5, cell viability continued to decline in all LNP-dsP21-322-2'F particle treatments (Figure 5d). Although differences in cell viability by LNP-dsCon-2'F were all generally nominal, treatments at 9 μ g/ml were found to be statistically significant for minimal reductions in cell viability on day 5 (Figure 5c,d).

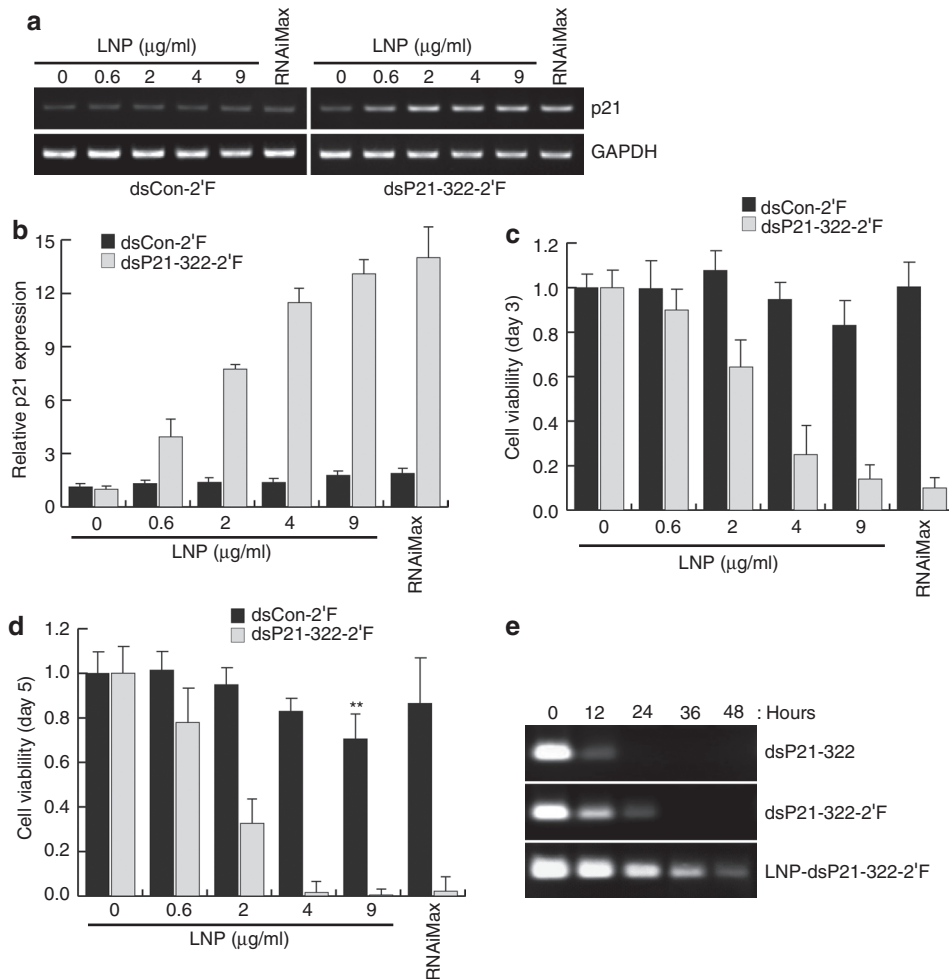


Figure 5 Lipidoid-mediated delivery of dsP21-322-2'F. (a) Duplexes were formulated into lipidoid-encapsulated nanoparticles (LNP). PC-3 cells were treated with the indicated quantities of LNP-dsCon-2'F or LNP-dsP21-322-2'F for 72 hours. Transfection of non-formulated dsCon-2'F or dsP21-322-2'F was performed using RNAiMax and served as controls for *in vitro* activity. Expression levels of p21 and GAPDH were assessed by semi-quantitative RT-PCR. (b) Relative expression of p21 was determined by real-time PCR (mean \pm SD from three independent experiments). Values of p21 were normalized to GAPDH. (c) Cell viability was quantified by MTS reagent 3 days following dsRNA treatments. Data is plotted as the mean \pm SD of three independent experiments relative to untreated cells (0 μ g/ml). (d) Cell viability at day 5 following dsRNA treatments. Statistical significance (** $P < 0.05$) of changes in cell viability by LNP-dsCon-2'F were determined by two-tailed *t*-test against untreated cells (0 μ g/ml). (e) Equal quantities of dsRNA were diluted in active mouse serum and incubated at 37 °C for the indicated lengths time. Duplex stability was visualized on an agarose gel. dsRNA, double-stranded RNA; GAPDH, glyceraldehyde 3-phosphate dehydrogenase; MTS, 3-(4,5-dimethylthiazol-2-yl)-5-(3-carboxymethoxyphenyl)-2-(4-sulfophenyl)-2H-tetrazolium; RT-PCR, reverse transcription-PCR.

Lipidoid-based particles can also increase the nuclease resistance of encapsulated siRNA molecules.³⁷ To test the effect of lipidoid formulation on dsP21-322-2'F stability, we evaluated the nuclease sensitivity of LNP-dsP21-322-2'F in active mouse serum. As shown in **Figure 5e**, LNP-dsP21-322-2'F was radically more stable than unmodified dsP21-322 or unformulated dsP21-322-2'F. Even at 48 hours, low levels of LNP-dsP21-322-2'F duplex remained detectable (**Figure 5e**). Quantification of duplex decay estimated the half-life of LNP-dsP21-322-2'F at ~38 hours (**Supplementary Figure S10**).

Lipidoid-formulated dsP21-322-2'F inhibits xenograft prostate tumor growth

To assess LNP-dsP21-322-2'F activity *in vivo*, homozygous athymic nude (nu/nu) male mice were subcutaneously

inoculated with PC-3 cells in their lower flanks. After 2 weeks when average tumor volume reached ~200 mm³, mice were randomly divided into four groups and treated with phosphate-buffered saline (PBS), LNP-dsCon-2'F, LNP-dsP21-322, or LNP-dsP21-322-2'F. Nanoparticles were administered *via* intratumoral injection at 5 mg/kg every 3 days for three total treatments (**Figure 6a**). Treatment with PBS served as a procedural control, while lipidoid-formulated dsP21-322 (LNP-dsP21-322) was utilized as a comparison treatment for LNP-dsP21-322-2'F. Xenografts were grown for a total of 36 days until animals in control groups met AVMA (America Veterinary Medical Association) guidelines for euthanasia as a result of tumor burden. All mice were subsequently euthanized and tumors surgically removed. Representative photographs of mice with subcutaneous masses and their

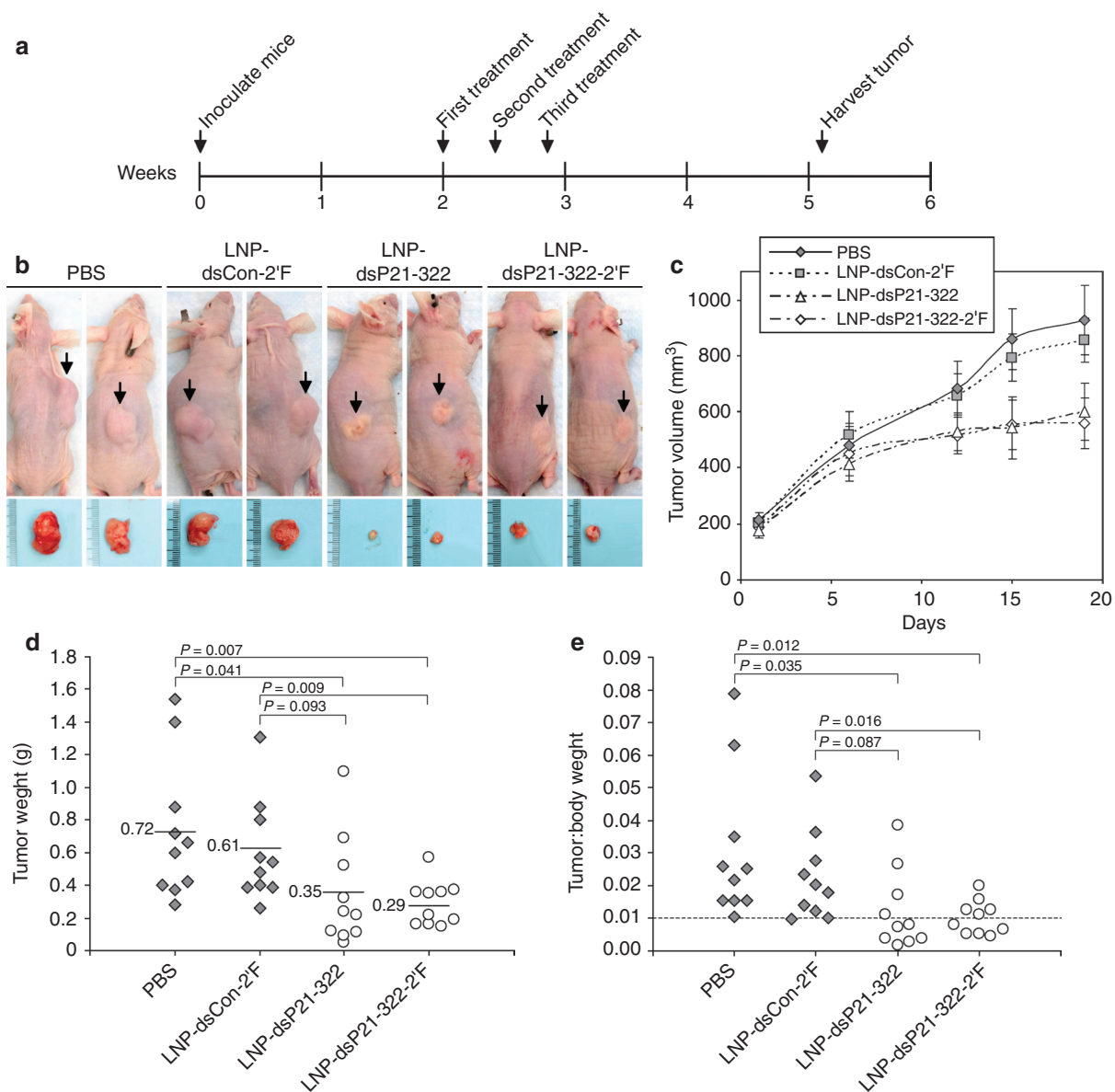


Figure 6 Reduction of xenograft prostate tumor growth by LNP-dsP21-322-2'F. (a) Experimental timeline and dosing schedule for mice treated with LNP-formulated dsRNA *via* intratumoral injection. The timeline corresponds to weeks following tumor inoculation. (b) Representative photographs of mice with subcutaneous masses (arrows) and corresponding tumors following surgical resection. Each tick mark on the ruler corresponds to 1 mm. (c) Subcutaneous tumor dimensions were recorded using calipers at the indicated time points following initial dsRNA treatment. Tumor volume was estimated using the modified ellipsoidal formula. Data is plotted as the mean volume \pm SD ($n = 10$ for each group). (d) Tumor weight was recorded at time of harvest and plotted according to treatment group. Mean tumor weight (g) and statistical significance is indicated. (e) Tumor-to-body weight ratio for each animal was plotted according to treatment group. A tumor-to-body weight ratio ≤ 0.01 signifies low tumor burden as delineated by the dotted line. Statistical analyses were calculated by two-tailed *t*-test between indicated groups. dsRNA, double-stranded RNA; LNP, lipidoid-encapsulated nanoparticles; PBS, phosphate-buffered saline.

corresponding tumors are indicated in **Figure 6b**. Tumor volume was also recorded periodically following initial treatments. As shown in **Figure 6c**, both LNP-dsP21-322 and LNP-dsP21-322-2'F treatment groups recorded reductions in xenograft volume compared to control groups. It is important to note that tumor volume was recorded using the modified ellipsoidal formula in which dimensions of only length and width were utilized to calculate tumor capacity. As tumor size visually depleted, white disc-like masses remained under the skin where the tumors once resided (**Figure 6b**). Because it

was unclear if this white subcutaneous tissue was still tumor, it was included in the measurements to calculate tumor volume. It was not until the tumors were excised that the white mass was revealed to be fatty and/or scarred tissue. As such, estimation of tumor volume was generous in regards to actual tumor size.

Further analysis of gross tumor weight revealed significant reductions in LNP-dsP21-322 and LNP-dsP21-322-2'F treatment groups compared to controls (**Figure 6d**). Tumor-to-body weight ratios were also significantly lower in LNP-dsP21-322

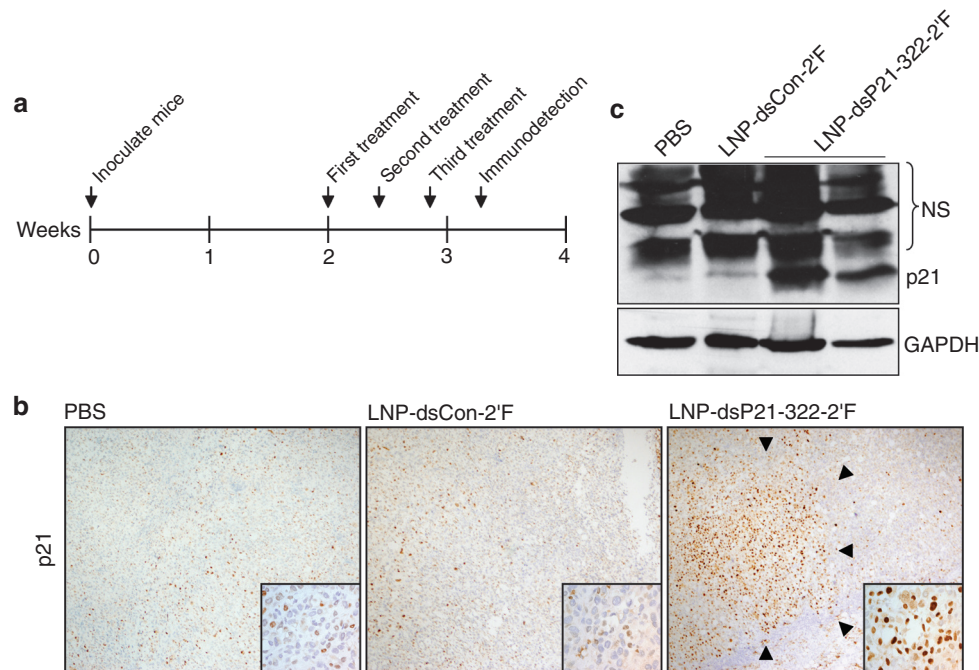


Figure 7 p21 induction by LNP-dsP21-322-2'F in xenograft prostate tumors. (a) Experimental timeline for immunodetection of p21 in xenograft prostate tumors. The timeline corresponds to weeks following tumor inoculation. (b) Representative microphotographs of p21 staining in tissue slides prepared from PBS, LNP-dsCon-2'F, and LNP-dsP21-322-2'F-treated xenografts. Arrow heads indicate area of intense staining in the LNP-dsP21-322-2'F-treated sample. Enlarged images show nuclear location of p21. (c) Whole tumor tissue was homogenized and p21 induction was confirmed by immunoblot analysis. Detection of GAPDH served as a loading control. Nonspecific (NS) protein bands also correspond with loading efficiency. Samples of LNP-dsP21-322-2'F treatments are from two separate tumors. GAPDH, glyceraldehyde 3-phosphate dehydrogenase; LNP, lipidoid-encapsulated nanoparticles; PBS, phosphate-buffered saline.

and LNP-dsP21-322-2'F treatment groups signifying a reduction in tumor burden (Figure 6e). It should be noted that the LNP-dsP21-322-2'F treatment group possessed less variation in tumor weight and burden compared to its unmodified form.

Immunohistochemistry (IHC) revealed that p21 was virtually undetectable in LNP-dsP21-322-2'F-treated xenografts ~3 weeks following initial doses (data not shown). Because of the reduction in tumor size, cells positive for p21 induction may have dissipated before analysis. To assess p21 activation *in vivo*, tumors were removed from mice 3 days following the final dose of lipidoid nanoparticles and processed for IHC (Figure 7a). As shown in Figure 7b, staining for p21 in control treatments was generally infrequent; any cells positive for p21 were randomly dispersed throughout the control tissues. In contrast, isolated areas of intense nuclear staining were detectable within the LNP-dsP21-322-2'F-treated xenografts. Increased levels of p21 were also detectable by immunoblot analysis in protein extracts prepared from total homogenized tissue (Figure 7c). These results suggest that p21 was activated *in vivo* by intratumoral delivery of LNP-dsP21-322-2'F.

Discussion

In the present study, we implement RNAa to explore the therapeutic potential of p21 induction in human prostate cancer xenografts by utilizing a lipidoid-based delivery vehicle. Lipidoid formulations are one of the leading materials for stabilizing and improving the bioavailability of siRNAs *in vivo*.^{5,6,37} Our results provide proof-of-principle that lipidoids are also

effective in delivering RNA duplex to facilitate p21 induction and inhibit prostate cancer cell growth.

In PC-3 cells, dsP21-322-2'F resulted in robust induction of p21 with corresponding reductions in Rb phosphorylation. Although Rb is an important mediator of p21, it is not the only means by which p21 can suppress cell growth. For example, p21 can inhibit proliferating cell nuclear antigen function and/or interfere with the activity of several oncogenic transcription factors (*i.e.*, E2F1, Myc, etc.).¹⁶ As such, induction of p21 by dsP21-322-2'F may have therapeutic benefit in cancer regardless of Rb status. In support, dsP21-322-2'F was capable of activating p21 and reducing viability in cell lines containing inactive (DU-145) or wild-type (PC-3 and LNCaP) Rb protein.

Although the growth inhibitory functions of dsP21-322-2'F depends on p21 induction, siP21 cotreatments did not completely restore PC-3 cells to a basal phenotype. For instance, siP21 appeared to only partially restore phosphorylated Rb levels to baseline and a significant fraction of sub-G1 cells remained in siP21 and dsP21-322-2'F cotreatments. Although these results may arise from the method utilized to compensate for p21 induction, it cannot rule out the possibility that some of the growth inhibitory functions of dsP21-322-2'F may result from nonspecific or off-target effects. Expression analysis of 12 additional cell cycle regulators and transcription factors revealed dsP21-322-2'F also deregulated CCNE1, p15, p27, and HDAC1. Presumably, activation of CCNE1 did not contribute to the growth arrest effects of dsP21-322-2'F; CCNE1 is known to accumulate in G1 phase to promote cell

cycle progression.³⁸ As such, its upregulation may indirectly result from dsP21-322-2'F-induced G1 arrest and/or accumulation of CDK inhibitors (*i.e.*, p21, p27, and p15). The downregulation of HDAC1 may have occurred through a canonical mechanism of RNAi; *in silico* analysis of the HDAC1 transcript reveals several possible sites semi-complementary to dsP21-322-2'F (data not shown). Previous studies have linked HDAC1 suppression to activation of CDK inhibitors (e.g., p21, p27, etc.).^{36,39,40} Although p21 induction was independent of HDAC1, its knockdown elevated p15 and p27 levels in PC-3 cells. This may suggest that activation of p15 and p27 by dsP21-322-2'F derives from HDAC1 depletion contributing, in part, to Rb hypophosphorylation and growth inhibition.

Characterization of off-target transcripts also indirectly evaluates target specificity. For instance, the expression of several key upstream regulators (*i.e.*, SP1, SP3, Myc, E2F1, and E2F3) were unaffected by dsP21-322-2'F removing them as candidates for modes of nonspecific gene induction. In addition, HDAC1 was determined to be reduced by dsP21-322-2'F; however, its selective knockdown had no impact on p21 expression. While dsP21-322-2'F possesses off-target activity, none of the evaluated genes accounted for p21 induction. Three additional dsRNAs (*i.e.*, dsP21-254, dsP21-280, and dsP21-402) were also determined to induce p21 expression by varying magnitudes. If taken into consideration that each activator possesses a different "seed" sequence and targets non-overlapping regions, the likelihood for each duplex functioning *via* suppression of nonspecific upstream regulators is potentially low.

Conventional RNAi requires high degrees of complementarity with the target transcript for effective cleavage and gene silencing.^{41,42} However, previous studies have concluded that cleavage of target molecule(s) may not be necessary for mechanisms of RNAa.^{15,43} In support, analysis of the mutant derivatives revealed that mismatches to the center of dsP21-322-2'F did not interfere with p21 induction, although sequence corresponding to the "seed" and 3'-flanking regions were essential for optimal function. Although cleavage activity may not be required for RNAa, extended complementarity in the 3'-flanking region is important for effective p21 induction by dsP21-322-2'F.

Concurrent use of both RNAi and RNAa may have cooperative effects in controlling cell phenotype. However, cotreatment with siRNA interfered with dsP21-322-2'F activity reducing its EC₅₀ by approximately tenfold. Competition between siRNAs has been reported in which delivery of multiple siRNAs hinders with the efficacy of the individual reagents.^{44,45} In this regards, co-delivery of multiple duplexes may similarly interfere with RNAa activity.

Being that p21 is seldom inactivated in human cancers, its upregulation may also benefit in treatment of other tumors.^{24–26} Lipidoid formulations are preferentially being developed to target the liver based on natural accumulation in hepatic tissue.⁵ In this regards, LNP-dsP21-322-2'F may have practical therapeutic application in liver cancer. In addition, it is quite possible that the other activators (dsP21-254, dsP21-280, and dsP21-402) may have therapeutic function in context to different cells, tissue, and/or cancer. However, caution may need to apply as p21 has been shown to correlate with nonconventional activities such as oncogenicity

under certain conditions. For example, overexpression of p21 in the cytoplasmic compartment has been associated with poor prognosis in select cancers.^{46–48} Although this function is less understood, its oncogenic activities may be dependent on nontraditional cytoplasmic targets of the protein. As such, features like localization and/or basal overexpression of p21 may need to be considered before therapeutic development in other cancers.

Lipidoid formulation of dsP21-322-2'F (LNP-dsP21-322-2'F) exhibited more consistent reduction in tumor size than its unmodified variant (LNP-dsP21-322). Perhaps, this may be attributed to the enhanced medicinal properties associated with dsP21-322-2'F. With a more refined treatment regime, the therapeutic efficacy of LNP-dsP21-322-2'F may be further enhanced in the xenograft model. For instance, long-term therapeutic application would benefit from recurring doses of LNP-dsP21-322-2'F. Additional chemical modifications would also be mandatory to further improve its medicinal properties. For instance, 2'-fluoro modification at additional positions may remove residual immunostimulatory effects. Although dsP21-322-2'F possesses off-target function, HDAC1 is a therapeutic target frequently overexpressed in numerous cancers types (e.g., prostate).^{40,49} Its knockdown may be a beneficial off-target consequence for inhibiting cancer cell growth.⁴⁰ Nonetheless, LNP-dsP21-322-2'F is a putative RNAa-based therapeutic with antitumor activity. Although lipidoids are preferentially utilized to target the liver, they may also function to deliver RNA duplexes locally to organs such as the prostate—accessible through a relatively small layer of soft tissue. LNP-dsP21-322-2'F may be administered with a small needle in a manner similar to the xenograft treatments and/or accompany biopsy procedures. However, improvement and/or discovery of novel *in vivo* delivery systems would ultimately benefit its therapeutic efficacy in prostate cancer. For instance, conjugation to an anti-PSMA aptamer may allow for systemic delivery of dsP21-322-2'F to PSMA-positive prostate cancer cells in a manner similar to siRNA-aptamer chimeras.⁵⁰ Our results demonstrate that lipidoid formulation can mediate RNAa both *in vitro* and *in vivo* by delivering dsP21-322-2'F to activate p21 expression and inhibit growth of prostate cancer cells. These findings suggest that RNAa in conjunction with lipidoids or other delivery systems may represent a novel therapeutic approach for enhancing endogenous gene expression and combating disease at the genetic level.

Materials and methods

Cell culture and dsRNA transfection. Human prostate cancer cell lines (PC-3, LNCaP, and DU-145) were maintained in RPMI 1640 medium supplemented with 10% fetal bovine serum, L-glutamine (2 mmol/l), penicillin (100 U/ml), and streptomycin (100 µg/ml) in a humidified atmosphere of 5% CO₂ at 37 °C. The day before dsRNA transfection, cells were plated in growth medium without antibiotics at a density of ~50–60%. Transfection of dsRNA was carried out using Lipofectamine RNAiMax (Invitrogen, Carlsbad, CA) according to the manufacturer's instructions. All duplexes were synthesized by Invitrogen and/or Alnylam Pharmaceuticals (Cambridge, MA). Production of 2'-fluoro-modified dsRNAs

were performed exclusively by Alnylam Pharmaceuticals. All dsRNA sequences are listed in Supplementary Table S1.

Cell stimulation and cytokine production. Whole blood from 3 anonymous donors was obtained from Research Blood Components (Brighton, MA) and pre-screened for infectious agents. Human peripheral blood mononuclear cells were isolated by *Ficoll* gradient centrifugation and plated in 96-well microplates at ~100,000 cells per well. Transfection of dsRNA was carried out using DOTAP (Roche, Indianapolis, IN) according to the manufacturer's protocol. Supernatants were harvested ~24 hours after transfection and immediately assayed for IFN- α and TNF- α production by ELISA (Bender Medsystems, Vienna, Austria). Each treatment was analyzed in triplicate for all three donors.

Establishing xenograft prostate tumors. All xenograft studies were performed according to protocol approved by the Institutional Animal Care and Use Committee (IACUC). PC-3 cells were cultured at a density of ~70–80% in 150 mm plates. Cells were trypsinized and centrifuged at 1,500 rpm for 5 minutes in complete medium. Cell pellets were subsequently washed and resuspended in PBS containing Matrigel (BD Biosciences, San Jose, CA) for *in vivo* inoculation. Homozygous athymic nude (nu/nu) male mice at 4–6 weeks of age were purchased from Simonsen Laboratories (Gilroy, CA). After 5 days of acclimation, animals were subcutaneously inoculated in their lower flanks with PC-3 cells (3×10^6) suspended in 0.2 ml of PBS containing Matrigel. Tumor volume was monitored by digital calipers and calculated using the modified ellipsoidal formula: tumor volume (mm^3) = (width) 2 \times length/2. Mice were examined weekly for body weight and overall health. The study ceased when the first animals met AVMA guidelines for euthanasia as a result of tumor burden.

Intratumoral delivery of lipidoid-formulated dsRNA. Two weeks after inoculation, tumor-bearing mice were randomly divided into four treatment groups (PBS, LNP-dsCon-2'F, LNP-dsP21-322, and LNP-dsP21-322-2'F) each containing 10–12 animals. Lipidoid-formulated dsRNA was administered *via* intratumoral injection at 5 mg/kg every 3 days for three total doses. PBS treatments were performed at volumes equivalent to LNP-dsP21-322-2'F doses. Sequences to all lipidoid-formulated dsRNAs are available in **Supplementary Table S1**.

Immunodetection in xenograft tissue. Mice were euthanized and tumors surgically resected according to protocols approved by the IACUC. Animals from treatment groups with more than 10 mice (PBS, LNP-dsCon-2'F, and LNP-dsP21-322-2'F) were killed early (3 days after final LNP dose) for prompt immunanalysis. Tumors from all remaining animals were harvested at the conclusion of the study. Each tumor was divided in half and placed in either radioimmunoprecipitation assay (RIPA) buffer containing protease inhibitors or 10% neutral buffered formalin for immunoblot analysis or IHC, respectively. The formalin-fixed tissue was eventually embedded in paraffin blocks, cut into 5 μm sections, and mounted onto glass slides. IHC was initiated by paraffin removal and rehydrating tissue sections in water. Slides were subsequently boiled in 10 mmol/l citrate, pH 6.0 for 15 minutes to improve

antigen recovery and treated with 3% hydrogen peroxide for 5 minutes. Afterward, sections were blocked in Tris-buffered saline (TBS) containing 0.1% Tween 20 and 5% goat serum for 1 hour. Immunodetection proceeded by incubating slides overnight at 4 °C with primary antibody specific to p21 (Cell Signaling Technology, Danvers, MA) diluted 1:500 in blocking solution. Slides were subsequently incubated with biotinylated secondary antibody and stained using the Elite ABC kit (Vector Laboratories, Burlington, CA) in conjunction with peroxidase substrate. An antibody specific to normal rabbit IgG (Cell Signaling Technology) was also utilized as a nonspecific control and generated no detectable staining. All slides were counterstained with hematoxylin.

Other experimental procedures are available in **Supplementary Materials and Methods**

Acknowledgments. This work was supported by funds from the National Cancer Institute (1R21CA131774-01), National Institutes of Health (1R01GM090293-0109), Department of Defense (W81XWH-08-1-0260), California Institute for Regenerative Medicine (RL1-00660-1), Special Program of Research Excellence (SPORE) in prostate cancer (P50CA89520), and Alnylam Pharmaceuticals. Alnylam Pharmaceuticals holds licenses for intellectual property related to the RNAa technology and lipidoid-based delivery system. RNA Therapeutics acknowledges having received funds from Alnylam Pharmaceuticals. R.M., M.M., K.C., and R.D. are employees at Alnylam Pharmaceuticals. R.F.P. is employed at RNA Therapeutics. All other authors declared no conflict of interest.

Supplementary material

Figure S1. 2'-fluoro-modification of dsP21-322.

Figure S2. Decay rates of dsP21-322 and dsP21-322-2'F in active mouse serum.

Figure S3. Sustained induction of p21 by dsP21-322-2'F correlates with impeded cell growth.

Figure S4. Activity of dsP21-322-2'F in different prostate cancer cell lines.

Figure S5. Sequence requirement of dsP21-322-2'F.

Figure S6. Phenotypic analysis of dsP21-322-2'F and its mutant derivatives.

Figure S7. Characterization of dsP21-322-2'F and siRNA cotreatments.

Figure S8. Nonspecific activities of dsP21-322-2'F.

Figure S9. Intracellular levels of dsP21-322-2'F.

Figure S10. Decay rate of LNP-dsP21-322-2'F in active mouse serum.

Table S1. Duplex RNAs and oligonucleotide sequences.

Materials and Methods.

1. Fire, A, Xu, S, Montgomery, MK, Kostas, SA, Driver, SE and Mello, CC (1998). Potent and specific genetic interference by double-stranded RNA in *Caenorhabditis elegans*. *Nature* **391**: 806–811.
2. Petrocca, F and Lieberman, J (2011). Promise and challenge of RNA interference-based therapy for cancer. *J Clin Oncol* **29**: 747–754.
3. Zimmermann, TS, Lee, AC, Akinc, A, Bramlage, B, Bumcrot, D, Fedoruk, MN et al. (2006). RNAi-mediated gene silencing in non-human primates. *Nature* **441**: 111–114.
4. Bisanz, K, Yu, J, Edlund, M, Spohn, B, Hung, MC, Chung, LW et al. (2005). Targeting ECM-integrin interaction with liposome-encapsulated small interfering RNAs inhibits the growth of human prostate cancer in a bone xenograft imaging model. *Mol Ther* **12**: 634–643.

5. Akinc, A, Goldberg, M, Qin, J, Dorkin, JR, Gamba-Vitalo, C, Maier, M et al. (2009). Development of lipidoid-siRNA formulations for systemic delivery to the liver. *Mol Ther* **17**: 872–879.
6. Akinc, A, Zumbuehl, A, Goldberg, M, Leshchiner, ES, Busini, V, Hossain, N et al. (2008). A combinatorial library of lipid-like materials for delivery of RNAi therapeutics. *Nat Biotechnol* **26**: 561–569.
7. Li, LC, Okino, ST, Zhao, H, Pookot, D, Place, RF, Urakami, S et al. (2006). Small dsRNAs induce transcriptional activation in human cells. *Proc Natl Acad Sci USA* **103**: 17337–17342.
8. Place, RF, Li, LC, Pookot, D, Noonan, EJ and Dahiya, R (2008). MicroRNA-373 induces expression of genes with complementary promoter sequences. *Proc Natl Acad Sci USA* **105**: 1608–1613.
9. Janowski, BA, Younger, ST, Hardy, DB, Ram, R, Huffman, KE and Corey, DR (2007). Activating gene expression in mammalian cells with promoter-targeted duplex RNAs. *Nat Chem Biol* **3**: 166–173.
10. Portnoy, V, Huang, V, Place, RF and Li, LC (2011). Small RNA and transcriptional upregulation. *Wiley Interdiscip Rev RNA* **2**: 748–760.
11. Huang, V, Qin, Y, Wang, J, Wang, X, Place, RF, Lin, G et al. (2010). RNAi is conserved in mammalian cells. *PLoS ONE* **5**: e8848.
12. Wang, J, Place, RF, Huang, V, Wang, X, Noonan, EJ, Magyar, CE et al. (2010). Prognostic value and function of KLF4 in prostate cancer: RNAi and vector-mediated overexpression identify KLF4 as an inhibitor of tumor cell growth and migration. *Cancer Res* **70**: 10182–10191.
13. Schwartz, JC, Younger, ST, Nguyen, NB, Hardy, DB, Monia, BP, Corey, DR et al. (2008). Antisense transcripts are targets for activating small RNAs. *Nat Struct Mol Biol* **15**: 842–848.
14. Morris, KV, Santoso, S, Turner, AM, Pastori, C and Hawkins, PG (2008). Bidirectional transcription directs both transcriptional gene activation and suppression in human cells. *PLoS Genet* **4**: e1000258.
15. Matsui, M, Sakurai, F, Elbashir, S, Foster, DJ, Manoharan, M and Corey, DR (2010). Activation of LDL receptor expression by small RNAs complementary to a noncoding transcript that overlaps the LDLR promoter. *Chem Biol* **17**: 1344–1355.
16. Abbas, T and Dutta, A (2009). p21 in cancer: intricate networks and multiple activities. *Nat Rev Cancer* **9**: 400–414.
17. Harper, JW, Elledge, SJ, Keyomarsi, K, Dynlacht, B, Tsai, LH, Zhang, P et al. (1995). Inhibition of cyclin-dependent kinases by p21. *Mol Biol Cell* **6**: 387–400.
18. Fang, L, Igarashi, M, Leung, J, Sugrue, MM, Lee, SW and Aaronson, SA (1999). p21Waf1/Cip1/Sdi1 induces permanent growth arrest with markers of replicative senescence in human tumor cells lacking functional p53. *Oncogene* **18**: 2789–2797.
19. Place, RF, Noonan, EJ and Giardina, C (2005). HDACs and the senescent phenotype of WI-38 cells. *BMC Cell Biol* **6**: 37.
20. Poole, AJ, Heap, D, Carroll, RE and Tyner, AL (2004). Tumor suppressor functions for the Cdk inhibitor p21 in the mouse colon. *Oncogene* **23**: 8128–8134.
21. Eastham, JA, Hall, SJ, Sehgal, I, Wang, J, Timme, TL, Yang, G et al. (1995). In vivo gene therapy with p53 or p21 adenovirus for prostate cancer. *Cancer Res* **55**: 5151–5155.
22. Wu, M, Bellas, RE, Shen, J and Sonenshein, GE (1998). Roles of the tumor suppressor p53 and the cyclin-dependent kinase inhibitor p21WAF1/CIP1 in receptor-mediated apoptosis of WEHI 231 B lymphoma cells. *J Exp Med* **187**: 1671–1679.
23. Sherr, CJ (1996). Cancer cell cycles. *Science* **274**: 1672–1677.
24. McKenzie, KE, Siva, A, Maier, S, Runnebaum, IB, Seshadri, R and Sukumar, S (1997). Altered WAF1 genes do not play a role in abnormal cell cycle regulation in breast cancers lacking p53 mutations. *Clin Cancer Res* **3**: 1669–1673.
25. Patiño-García, A, Sotillo-Piñeiro, E and Sierrasesúmaga-Aríznavarreta, L (1998). p21WAF1 mutation is not a predominant alteration in pediatric bone tumors. *Pediatr Res* **43**: 393–395.
26. Shiohara, M, el-Deiry, WS, Wada, M, Nakamaki, T, Takeuchi, S, Yang, R et al. (1994). Absence of WAF1 mutations in a variety of human malignancies. *Blood* **84**: 3781–3784.
27. Chen, Z, Place, RF, Jia, ZJ, Pookot, D, Dahiya, R and Li, LC (2008). Antitumor effect of dsRNA-induced p21(WAF1/CIP1) gene activation in human bladder cancer cells. *Mol Cancer Ther* **7**: 698–703.
28. Whitson, JM, Noonan, EJ, Pookot, D, Place, RF and Dahiya, R (2009). Double stranded-RNA-mediated activation of P21 gene induced apoptosis and cell cycle arrest in renal cell carcinoma. *Int J Cancer* **125**: 446–452.
29. Morris, KV, Chan, SW, Jacobsen, SE and Looney, DJ (2004). Small interfering RNA-induced transcriptional gene silencing in human cells. *Science* **305**: 1289–1292.
30. Bumcrot, D, Manoharan, M, Koteliensky, V and Sah, DW (2006). RNAi therapeutics: a potential new class of pharmaceutical drugs. *Nat Chem Biol* **2**: 711–719.
31. Place, RF, Noonan, EJ, Földes-Papp, Z and Li, LC (2010). Defining features and exploring chemical modifications to manipulate RNAi activity. *Curr Pharm Biotechnol* **11**: 518–526.
32. Rubin, SJ, Hallahan, DE, Ashman, CR, Brachman, DG, Beckett, MA, Virudachalam, S et al. (1991). Two prostate carcinoma cell lines demonstrate abnormalities in tumor suppressor genes. *J Surg Oncol* **46**: 31–36.
33. Hornung, V, Guenther-Biller, M, Bourquin, C, Ablasser, A, Schlee, M, Uematsu, S et al. (2005). Sequence-specific potent induction of IFN- α by short interfering RNA in plasmacytoid dendritic cells through TLR7. *Nat Med* **11**: 263–270.
34. Judge, AD, Bola, G, Lee, AC and MacLachlan, I (2006). Design of noninflammatory synthetic siRNA mediating potent gene silencing in vivo. *Mol Ther* **13**: 494–505.
35. Gartel, AL and Tyner, AL (1999). Transcriptional regulation of the p21(WAF1/CIP1) gene. *Exp Cell Res* **246**: 280–289.
36. Zupkovitz, G, Grausenburger, R, Brunmeir, R, Senese, S, Tischler, J, Jurkin, J et al. (2010). The cyclin-dependent kinase inhibitor p21 is a crucial target for histone deacetylase 1 as a regulator of cellular proliferation. *Mol Cell Biol* **30**: 1171–1181.
37. Semple, SC, Akinc, A, Chen, J, Sandhu, AP, Mui, BL, Cho, CK et al. (2010). Rational design of cationic lipids for siRNA delivery. *Nat Biotechnol* **28**: 172–176.
38. Möröy, T and Geisen, C (2004). Cyclin E. *Int J Biochem Cell Biol* **36**: 1424–1439.
39. Noonan, EJ, Place, RF, Basak, S, Pookot, D and Li, LC (2010). miR-449a causes Rb-dependent cell cycle arrest and senescence in prostate cancer cells. *Oncotarget* **1**: 349–358.
40. Noonan, EJ, Place, RF, Pookot, D, Basak, S, Whitson, JM, Hirata, H et al. (2009). miR-449a targets HDAC-1 and induces growth arrest in prostate cancer. *Oncogene* **28**: 1714–1724.
41. Elbashir, SM, Martinez, J, Patkaniowska, A, Lendeckel, W and Tuschl, T (2001). Functional anatomy of siRNAs for mediating efficient RNAi in Drosophila melanogaster embryo lysate. *EMBO J* **20**: 6877–6888.
42. Martinez, J, Patkaniowska, A, Urlaub, H, Lührmann, R and Tuschl, T (2002). Single-stranded antisense siRNAs guide target RNA cleavage in RNAi. *Cell* **110**: 563–574.
43. Chu, Y, Yue, X, Younger, ST, Janowski, BA and Corey, DR (2010). Involvement of argonaute proteins in gene silencing and activation by RNAs complementary to a non-coding transcript at the progesterone receptor promoter. *Nucleic Acids Res* **38**: 7736–7748.
44. Bitko, V, Musiyenko, A, Shulyayeva, O and Barik, S (2005). Inhibition of respiratory viruses by nasally administered siRNA. *Nat Med* **11**: 50–55.
45. Hutvagner, G, Simard, MJ, Mello, CC and Zamore, PD (2004). Sequence-specific inhibition of small RNA function. *PLoS Biol* **2**: E98.
46. Winters, ZE, Leek, RD, Bradburn, MJ, Norbury, CJ and Harris, AL (2003). Cytoplasmic p21WAF1/CIP1 expression is correlated with HER-2/ neu in breast cancer and is an independent predictor of prognosis. *Breast Cancer Res* **5**: R242–R249.
47. Shiraki, K and Wagayama, H (2006). Cytoplasmic p21(WAF1/CIP1) expression in human hepatocellular carcinomas. *Liver Int* **26**: 1018–1019.
48. Xia, W, Chen, JS, Zhou, X, Sun, PR, Lee, DF, Liao, Y et al. (2004). Phosphorylation/cytoplasmic localization of p21Cip1/WAF1 is associated with HER2/neu overexpression and provides a novel combination predictor for poor prognosis in breast cancer patients. *Clin Cancer Res* **10**: 3815–3824.
49. Weichert, W, Röske, A, Gekeler, V, Beckers, T, Stephan, C, Jung, K et al. (2008). Histone deacetylases 1, 2 and 3 are highly expressed in prostate cancer and HDAC2 expression is associated with shorter PSA relapse time after radical prostatectomy. *Br J Cancer* **98**: 604–610.
50. Dassie, JP, Liu, XY, Thomas, GS, Whitaker, RM, Thiel, KW, Stockdale, KR et al. (2009). Systemic administration of optimized aptamer-siRNA chimeras promotes regression of PSMA-expressing tumors. *Nat Biotechnol* **27**: 839–849.



Molecular Therapy: Nucleic Acids is an open-access journal published by Nature Publishing Group. This work is licensed under the Creative Commons Attribution-NonCommercial-No Derivative Works 3.0 Unported License. To view a copy of this license, visit <http://creativecommons.org/licenses/by-nc-nd/3.0/>

Supplementary Information accompanies this paper on the Molecular Therapy: Nucleic Acids website (<http://www.nature.com/mtna>)